Electronic supplementary material

Insect mitochondria as targets of freezing-induced injury.

Štětina T., Des Marteaux L.E., Koštál V.

List of materials:

Supplementary methods

Citrate synthase activity assay

Total proteins were extracted from three biological replicates (each comprising 10 pooled dissected fat bodies) in 50 mM Tris buffer, pH 8.0, containing 0.2 M sucrose, 1 mM EDTA, and 1% Triton X. The activity of CS in the protein extracts was followed after addition of two substrates (0.15 mM acetyl CoA and 0.25 mM oxaloacetate) by measuring the formation of the mercaptid ion released from acetyl CoA-SH by use of the 0.05 mM DTNB reagent (5,5'-dithiobis-2-nitrobenzoic acid) and monitoring the absorbance at 412 nm. The enzyme CS is located at the mitochondria matrix, and is the first step of Krebs cycle catalyzing the condensation reaction of acetate and oxaloacetate to form citrate.

Mitochondrial/nuclear DNA relative quantification

Total DNA was extracted from four biological replicates (each comprising 50 pooled whole larvae) using RNA Blue reagent (TopBio, Vestec, Czech Republic) according to manufacturer's instructions. Pelleted total DNA was dissolved in 8 mM NaOH, pH 8.0, levelled to concentration 0.05 μg DNA/1μL, and 2 μL aliquots of DNA solution were used for quantitative real-time PCR (qPCR) on a CFX96 PCR cycler (BioRad, Philadelphia, PA, USA) to amplify DNA products from genes coding for cytochrome c-oxidase I (*COX I*, mitochondrial gene), and ribosomal protein 19 (*RpL19*, nuclear gene). The PCR reaction was composed of 2 μL DNA template, 17.2 μL LA Hot Start Plain Master Mix (TopBio), and 0.4 μL of each PCR primer at a final concentration 0.4 μM. PCR primer sequences were: *COX I* forward: ACAACGTCAAGTAATTTATCCTGTCCA; *COX I* reverse: GCTATGTTCAGCTGGGGGTG (79 bp-long amplicon); *Rp19* forward*:* CCGAGAAGCAGCGCAGTAAA; *Rp19* reverse: CTTGGCGTGCAGAGCGATAA (131 bp-long amplicon) (all primer sequences shown in 5'→3' direction). The PCR conditions were: initial denaturation at 95°C/3 min, followed by 40 cycles of denaturation at 94°C/30 sec, annealing at 61°C/30 sec, and extension at 72°C/30 sec, followed by final extension at 72°C/1 min. The melting analysis and running PCR reactions on agarose gels confirmed that unique DNA products of expected size were amplified. The relative abundance of mitochondrial/nuclear DNA was estimated as the ratio *COX I* Eff ^{Ct} */ RpL19* Eff ^{Ct}, where Eff is the efficiency of PCR amplification (1.85) and Ct is the qPCR critical cycle.

Processing of pre-fixed tissues for TEM

After washing in PBS, we continued in fixation using 2% OsO_4 (EMS, Hatfield, Pennsylvania) in PBS for 2 h, washing in PBS, dehydration in grading acetone solutions (30→50→70→80→90→95→100% in 15 min intervals), and embedding into resin Embed-812 (EMS):acetone grading from 1:2, 1:1, 2:1, 1:0 (pure resin) in 1 h intervals. After complete dehydration, the resin was polymerized at 60°C/24 h and the blocks were sectioned using an ultramicrotome Leica UC6 (Leica microsystems GmbH, Wetzlar, Germany) equipped with DiATOME diamond knife (EMS). The ultra-thin sections (70 nm) were placed on 300-mesh-Cu grids and counter-stained with saturated ethanolic uranyl acetate for 30 min, followed by lead citrate for 20 min. The grids with sections were then coated by carbon film using JEOL JE 4C coater (JEOL, Tokio, Japan), and micrographs were taken by a transmission electron microscope, JEOL JEM - 1010 1 (JEOL, Tokio, Japan).

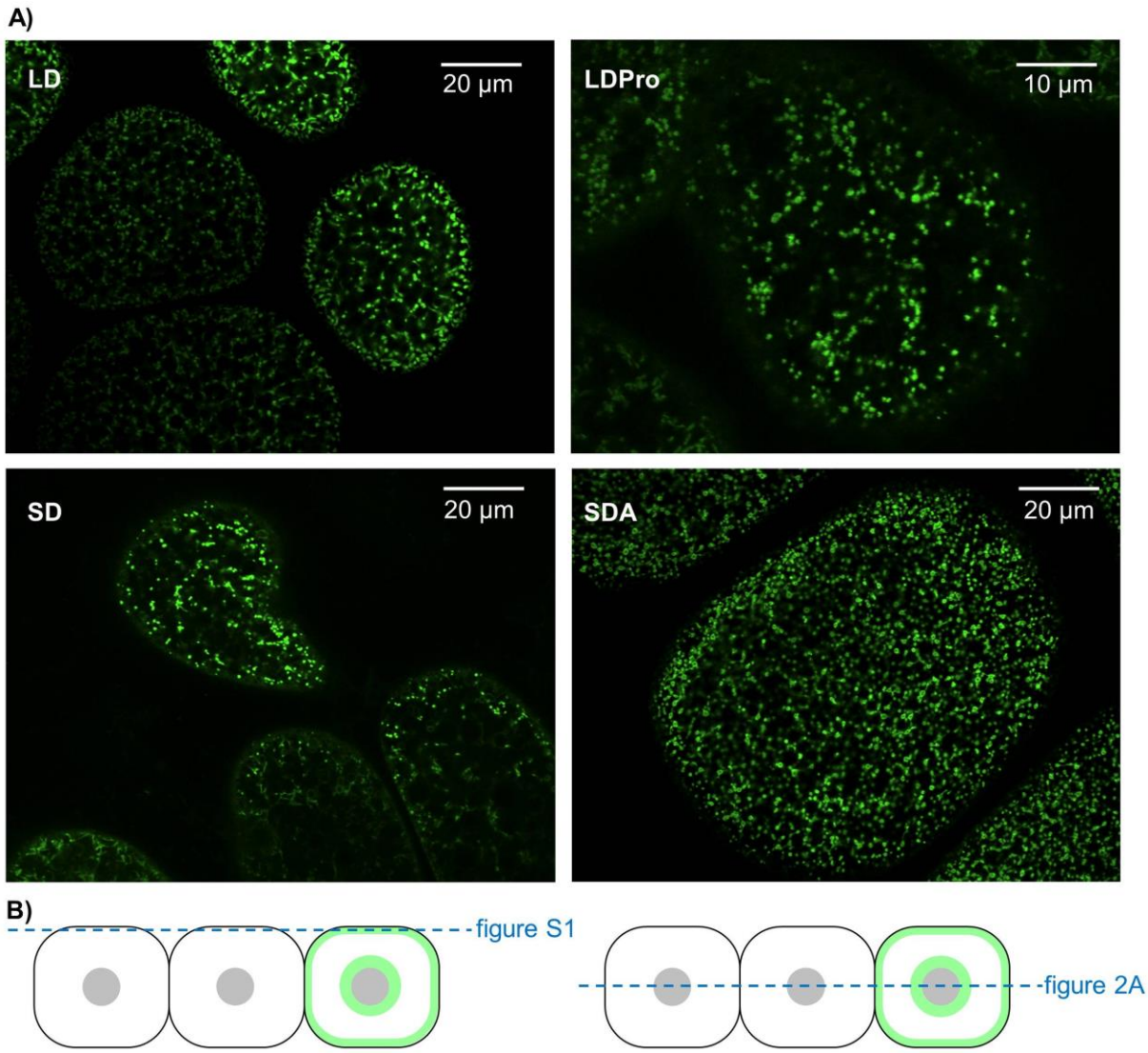

Figure S1. Staining of mitochondria in fat body tissue – MitoTracker Green.

(**A**) The fat body tissues from four phenotypic variants of *C. costata* larvae (LD, LDPro, SD, and SDA) and stained using green-fluorescent mitochondrial stain MitoTracker Green (ThermoFisher Scientific, Waltham, MA, USA) as follows: fat bodies were dissected into chilled Schneider's Drosophila Medium (Biosera, Nuaillé, France) containing 500 nM MitoTracker Green and held in the dark at 30°C for 30 min. Fat bodies were then washed three times in fresh Schneider's, placed on slides in a droplet of Schneider's medium, and imaged immediately on a Confocal Olympus FluoView FV1000 microscope system (Olympus Europa) at 100 × magnification with excitation/emission wavelengths of 488/520 nm.Two main populations of mitochondria were distributed around the nucleus and close the cell periphery (see green areas in the schematic drawing). This figure (S1) shows representative micrographs where the optical sections were taken close to the surface of fat body tissue so that the micrographs show the peripheral populations of mitochondria. In contrast, Figure 2A in the main text shows the optical sections taken close the midline of fat body tissue where the nuclei are located. (**B**) The MitoTracker Green signal was variable in different parts of fat body tissue and different cells (irrespective of the optical section taken). The variability in mitochondrial distribution between and inside cells did not allow us to use the MitoTracker Green signal for exact quantification of mitochondrial counts.

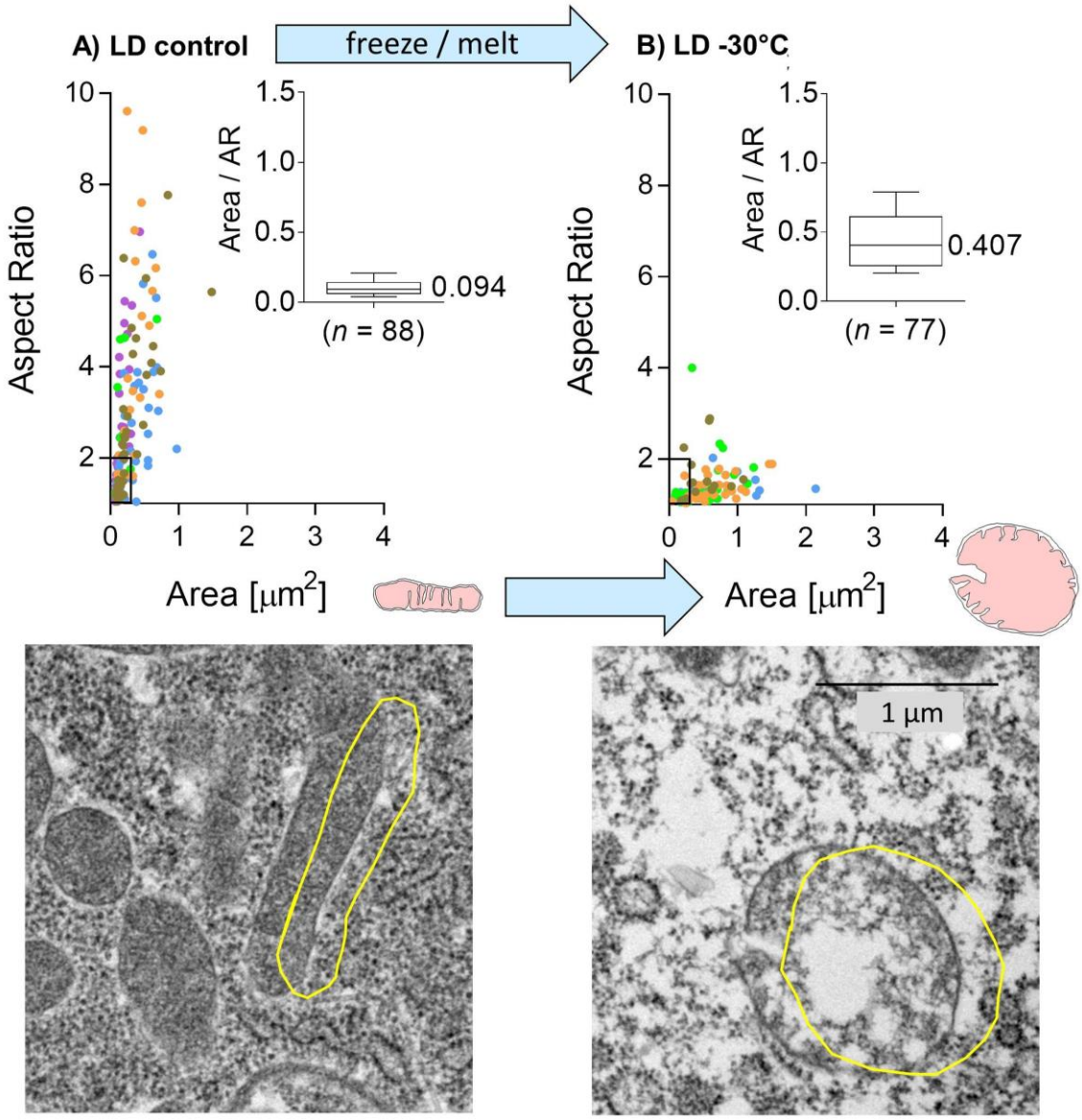

Figure S2. Analysis of mitochondrial shape – ImageJ.

Example analysis of mitochondrial shapes in two larvae: (**A**) LD control larva (not exposed to cold stress), and (**B**) LD larva exposed to freezing stress at -30°C. Each coloured dot represents a result of shape analysis of a single mitochondrion. Differently coloured dots mean different fat body cells of the same larva. Representative TEM micrographs of two mitochondria taken at 25,000 x magnification are shown (all TEM micrographs are available upon request). The hand-drawn yellow lines delineating the mitochondria are slightly offset for better clarity. Two parameters were calculated by ImageJ and plotted: *x axis*: Area ─ the surface area of mitochondrial section in μm^2; and *y axis*: Aspect Ratio (AR) ─ the ratio of major/minor axis of fitted ellipse. Rectangles in the lower left parts of plotting areas delimit very small mitochondria (*x*, Area up to 0.2 μm^2; *y*, AR up to 2) that were systematically excluded from further analysis as they most likely represent cuts close to the mitochondrial periphery/tip. In order to obtain a single 'master' descriptor of mitochondrial shape, we next calculated the ratio Area/AR for each mitochondrion and the median Area/AR ratio for each larva (biological replicate) was taken for statistical analysis of differences in mitochondrial shape between phenotypic variants. The inset diagrams show medians (line with number), upper and lower quartiles (box), 5% and 95% percentiles (whiskers) of Area/AR values for *n* mitochondria analyzed in each larva. The results of ImageJ analysis of all fat body (3,468) and hindgut (4,393) mitochondria are shown in datasets S1 and S2, respectively.

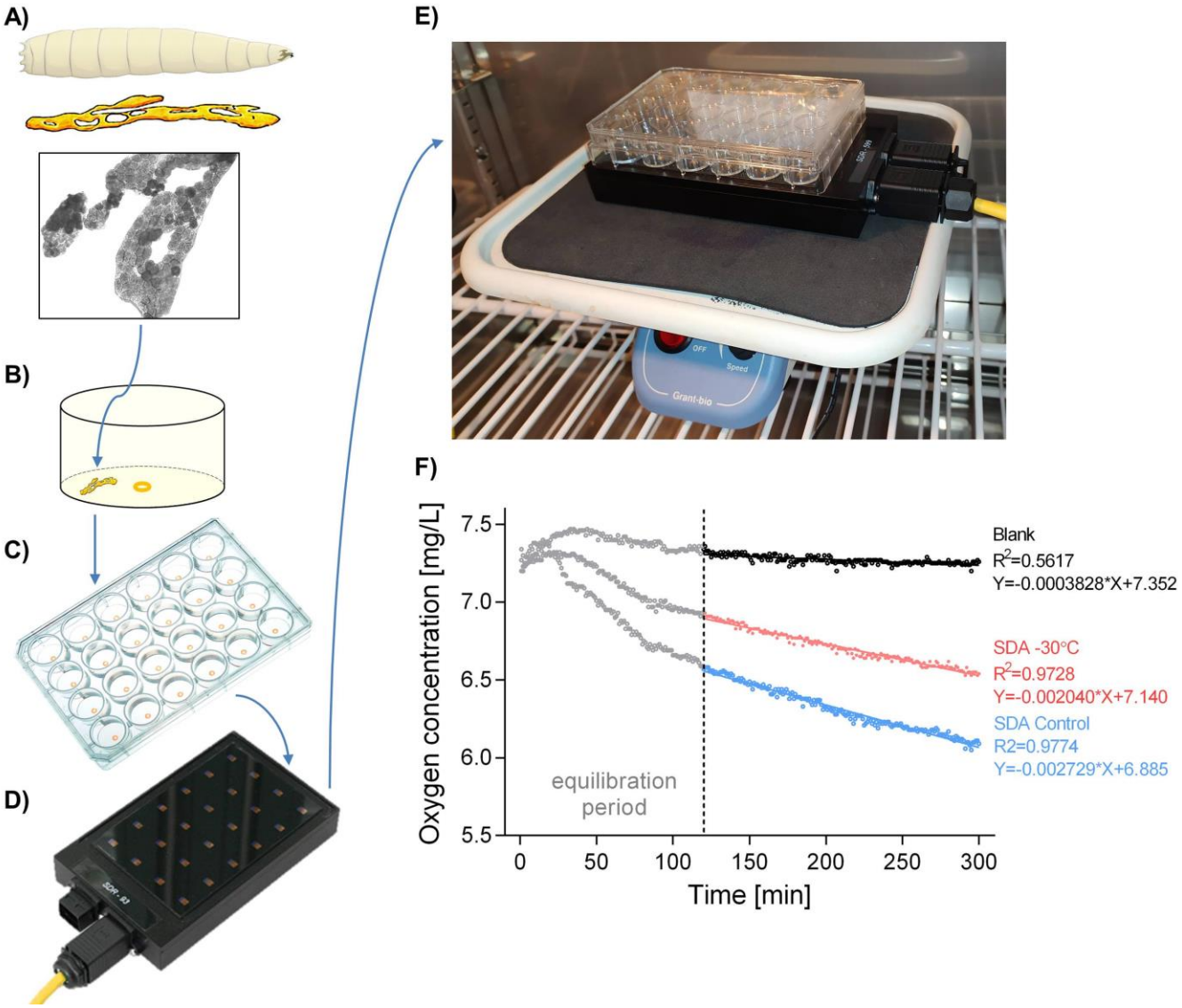

Figure S3: Analysis of oxygen consumption in dissected fat body tissues – PreSens.

(**A**) The fat body tissues were dissected in PBS from 20 *C. costata* larvae, pooled and transferred immediately to (**B**) 3.2 mL of Schneider's Drosophila Medium saturated with air (pipette pumping) in the wells of the (**C**) disposable 24-Well Plate for Online Oxygen Monitoring OxoDish® OD24 (PreSens). For each treatment, four to eight biological replicates (wells, each containing 20 tissues) were measured. The plate was closed and situated on (**D**) Multiwell Plate SD SensorDish Reader (PreSens), sitting on (**E**) PS-3D fixed-tilt platform rotator (Grant Instruments, Cambridge, UK) set to 5 rpm, and whole setup was housed in MIR 154 incubator set to 23°C. The plates were allowed to equilibrate for 120 min and then, a decrease of oxygen concentration over time was measured for 180 min in 1 min intervals. Finally, the rate of oxygen consumption in pmol/min/tissue was calculated from the slope of fitted linear curves using software SDR v4.1.0 (PreSens). (**F**) Three examples of PreSens records representing the decrease of oxygen concentration in three wells: Blank (no tissues, just Schneider's medium, black symbols. This rate was considered as background (Bckgr.) and subtracted from tissue samples), SDA Control (tissues dissected from control larvae not exposed to stress, blue symbols), and SDA -30°C (tissues dissected from larvae exposed to freezing stress at -30°C, red symbols). The linear regressions are fitted to data taken over the 3-h-long interval (120 – 300 min).

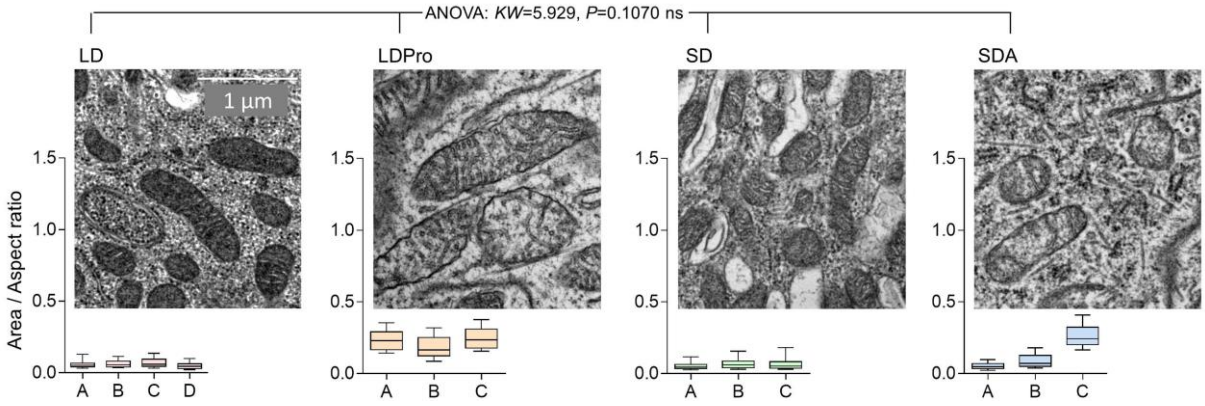

Figure S4. Effect of acclimation on hindgut mitochondrial morphology – TEM.

Representative TEM micrographs of hindgut mitochondria in *C. costata* larvae of four acclimation variants (LD, LDPro, SD, SDA, see Figure 1). All micrographs were taken at 25,000 x magnification. Mitochondrial shape was analyzed as explained in Figure S2 and the raw dataset of all mitochondrial parameters can be found in Dataset S2. The box plots below each micrograph show distributions (median, quartiles, 5% and 95% percentiles) of mitochondrial shapes in individual larvae (A to D). The distributions did not pass D'Agostino & Pearson omnibus normality tests and, therefore, the differences in mitochondrial shape between acclimation variants were analyzed using nonparametric Kruskal-Wallis test (*KW* statistics and *P*-value shown).

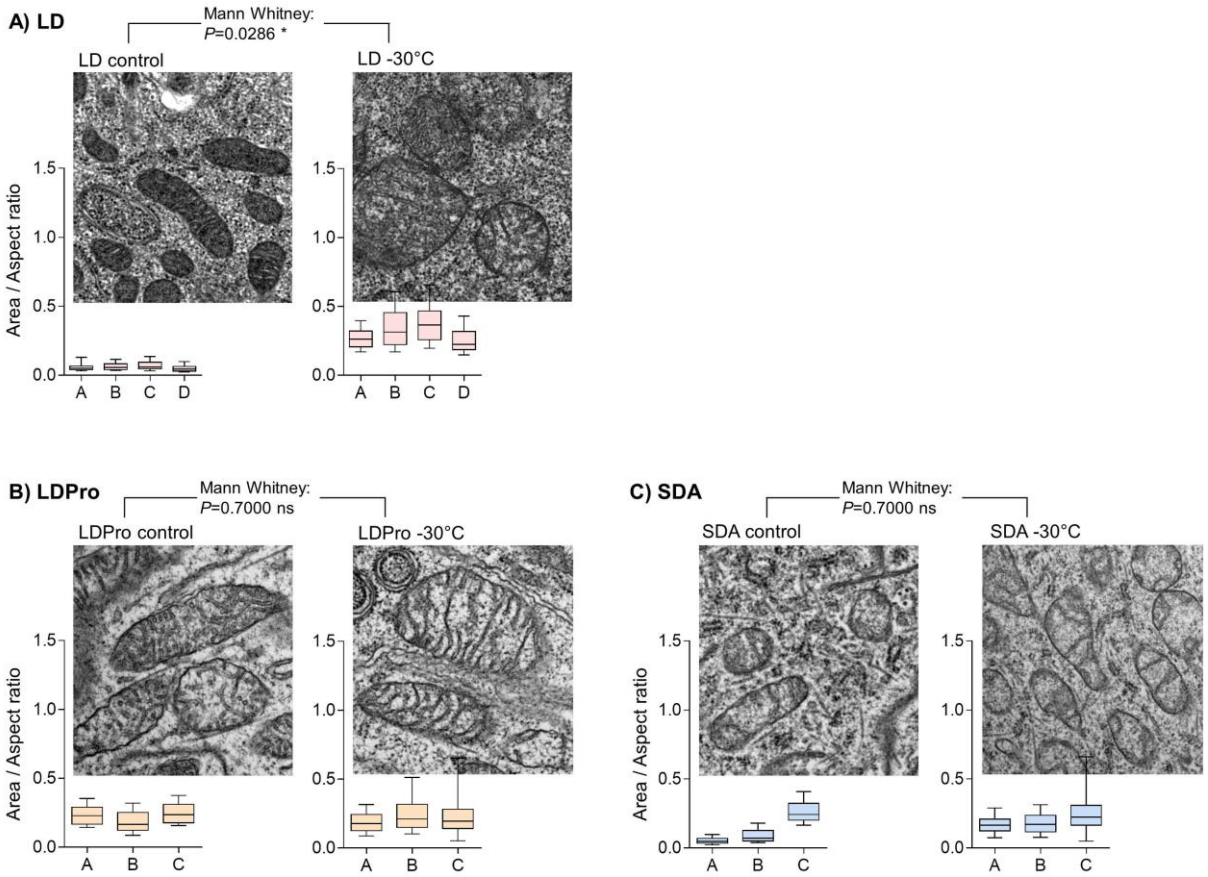

Figure S5. Effect of freezing stress on hindgut mitochondrial morphology – TEM.

Representative TEM micrographs of hindgut mitochondria in *C. costata* larvae exposed to freezing stress (-30°C) and appropriate controls (non-frozen). Three acclimation variants were assayed: (**A**) LD, (**B**) LDPro, and (**C**) SDA (see Figure 1). All micrographs were taken at 25,000 x magnification. Mitochondrial shape was analyzed as explained in Figure S2 and the raw dataset of all mitochondrial parameters can be found in Dataset S2. The box plots below each micrograph show distributions (median, quartiles, 5% and 95% percentiles) of mitochondrial shapes in individual larvae (A to D). The distributions did not pass D'Agostino & Pearson omnibus normality tests and, therefore, the differences in mitochondrial shape between control and frozen larvae were analyzed using nonparametric Mann Whitney tests (*P*-values shown).